Available online at www.sciencedirect.com
ScienceDirect
Advanced Drug Delivery Reviews 59 (2007) 1036–1053
Advanced DRUG DELIVERY Reviews
www.elsevier.com/locate/addr

A cell cycle automaton model for probing circadian patterns of anticancer drug delivery ☆

Atilla Altinok [a], Francis Lévi [b,c,d], Albert Goldbeter [a,*]

[a] *Unité de Chronobiologie théorique, Faculté des Sciences, Université Libre de Bruxelles, Campus Plaine, C.P. 231, B-1050 Brussels, Belgium*
[b] *INSERM, U776, Rythmes Biologiques et Cancers, Villejuif, F-94807, France*
[c] *Université Paris-Sud, UMR-S0776, Orsay, F-91405, France*
[d] *Assistance Publique-hôpitaux de Paris, Unité de Chronothérapie, Département de Cancérologie, hôpital Paul Brousse, Villejuif, F-94807, France*

Received 18 July 2006; accepted 25 September 2006
Available online 28 June 2007

Abstract

To optimize the temporal patterning of drug delivery used in cancer chronotherapy, we resort to an automaton model describing the transitions through the successive phases of the cell cycle. The model accounts for the progressive desynchronization of cells due to the variability of the durations of the cell cycle phases, and for the entrainment of the cell cycle by the circadian clock. Focusing on the cytotoxic effect of the anticancer drug 5-fluorouracil (5-FU), which kills cells in the S phase, we compare the effect of continuous infusion of 5-FU with various circadian patterns of 5-FU administration that peak either at 4 a.m., 10 a.m., 4 p.m., or 10 p.m. The model indicates that the cytotoxic effect of 5-FU is minimum for the circadian delivery peaking at 4 a.m., and maximum for the continuous infusion or the circadian pattern peaking at 4 p.m. These results fit well with experimental observations and illustrate how the modeling approach based on the cell cycle automaton may help to predict the cytotoxic effect of anticancer drugs affecting various phases of the cell cycle.

Keywords: Chronotherapy; Chronopharmacology; Anticancer medications; Circadian rhythm; Cell cycle model

Contents

☆ This review is part of the *Advanced Drug Delivery Reviews* theme issue on "Chronobiology, Drug Delivery and Chronotherapeutics".

* Corresponding author. Tel.: +32 2 650 5772; fax: +32 2 650 5767.
E-mail address: agoldbet@ulb.ac.be (A. Goldbeter).

0169-409X/$ - see front matter © 2007 Elsevier B.V. All rights reserved.
doi:10.1016/j.addr.2006.09.022

1. Introduction

Recent experimental studies have established a link between circadian rhythms and tumor progression. Thus, the rate of tumor growth in rodents increases as a result of mutations affecting the circadian clock [1] and of disruption of the neural pacemaker governing circadian rhythms [2]. A rationale for these findings is provided by the demonstration that the cell cycle is directly controlled by the circadian clock [3–5]. This explains why progression through the cell cycle and variation of key cell cycle components often display a strong circadian dependence [6–9]. The link between the circadian clock and cancer is further illustrated by the effect of circadian rhythms on a variety of anticancer medications [10–12]. Circadian rhythms affect the patient tolerance to these medications and their efficacy by modulating their metabolism and cell cycle dynamics. Each cancer medication is characterized, during the 24-hour period, by a specific pattern of tolerance (chronotolerance) and efficacy (chronoefficacy) [12].

Anticancer medications generally exert their effect by interfering with the cell division cycle, often by blocking it at a specific phase. Thus, anticancer drugs exert most of their cytotoxicity on dividing cells through interactions with cell cycle or apoptosis-related targets [10–14]. Antimetabolites, such as 5-fluorouracil (5-FU), are primarily toxic to cells that are undergoing DNA synthesis, i.e., during the S phase, while antimitotic agents, such as vinorelbine or docetaxel, are primarily toxic to cells that are undergoing mitosis, during the M phase. Conversely, alkylating agents such as cyclophosphamide or platinum complexes, seldom display any cell cycle phase specificity; thus, cellular metabolism and detoxification processes play a major role in the cell kill mechanisms of these therapeutic agents. The phases of the cell cycle during which the various classes of anticancer drugs act are summarized in Fig. 1. In addition, the pharmacokinetics of a medication and its metabolites determine the cell exposure dynamics that will result in the drug-induced cell damage.

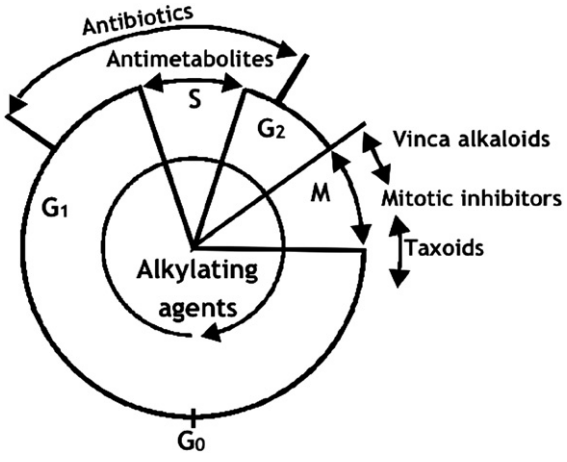

Fig. 1. Schematic representation of the phase(s) at which various classes of anticancer drugs act on the cell cycle. The anticancer drug 5-FU considered in this paper is an antimetabolite that interferes with DNA replication and acts on cells in S phase.

The marked influence of circadian rhythms on chronotolerance and chronoefficacy has motivated the development of chronotherapeutic approaches, particularly in the field of cancer [10–14]. Assessing the effectiveness of various temporal schedules of drug delivery is central to cancer chronotherapeutics. Modeling tools can help to optimize time-patterned drug administration to increase effectiveness and reduce toxicity [15]. To assess the effect of the circadian delivery of anticancer drugs by means of modeling and numerical simulations requires a model for the cell cycle. Different models for the cell cycle have been proposed. The complexity of these models increases as the number of molecular details is added [16–19]. An alternative, pragmatic approach shuns the molecular details and relies on a simple phenomenological description of the cell cycle in terms of an automaton, which switches between sequential states corresponding to the successive phases of the cell cycle. In this model, the transition between some phases of the cell cycle, i.e., cell cycle progression or exit from the cycle, is affected by the presence of anticancer medications. The cell cycle automaton model is based on the perspective that the transitions between the various phases of the cell cycle entail a random component [20–22]; this model is directly inspired by our previous study of a follicular automaton model for the growth of human hair follicles [23,24]. The model allows us to investigate how different temporal patterns of drug administration affect cell proliferation.

To illustrate the use of the cell cycle automaton model, herein we focus on the chronotherapeutic scheduling of 5-fluorouracil (5-FU), a reference drug for treating gastrointestinal, breast, and various other cancers. The half-life of this medication is 10–20 min; thus, the exposure pattern matches rather well its chronotherapeutic drug-delivery schedule [25], which will be the only one considered here. S-phase cells exposed to 5-FU arrest in S phase as a result of thymidilate synthase inhibition; then, they progress through the cell cycle or die through p53-dependent or independent apoptosis. A marked chronopharmacology of 5-FU has been demonstrated, both in experimental models and in cancer patients [26]. These data led to the development of intuitive chronomodulated delivery schedules aiming to minimize the toxic effects of 5-FU on healthy cells through its nighttime, rather than daytime, infusion. The most widely used chronomodulated schedule of 5-FU involves the sinusoidal modulation of its delivery rate between 10 p.m. to 10 a.m., with a peak at 4 a.m., in diurnally active cancer patients. This scheme improves patient 5-FU tolerability up to five-fold as compared to constant-rate infusion and makes possible a 40% increase in the tolerable dose and the near-doubling of antitumor activity in patients with metastatic colorectal cancer [27,28]. The 5-FU chronomodulated schedule, with peak delivery rate at 4 a.m., also is much less toxic than other circadian semi-sinusoidal schedules that utilize peak delivery rates that differ from 4 a.m. by 6 to 12 h.

Herein, we resort to the automaton model for the cell cycle to investigate the comparative effectiveness of different chronomodulated schedules of 5-FU administration. The analysis brings to light the importance of the circadian time of the peak in 5-FU as well as the effect of the variability in cell

cycle phase durations in determining the response to this antiproliferative drug. The results explain why the least toxic schedule of 5-FU delivery for diurnally active cancer patients is a circadian modulated drug-administration pattern that peaks at 4 a.m., and why the most cytotoxic schedule is either a circadian modulated drug-administration pattern that peaks at 4 p.m. or a continuous (non-varying-in-time) constant 24-hour infusion. The approach presented here can readily be extended to other types of anticancer drugs acting upon different stages of the cell cycle.

2. An automaton model for the cell cycle

The automaton model for the cell cycle (Fig. 2) is based on the following assumptions:

1) The cell cycle consists of four successive phases along which the cell progresses: G1, S (DNA replication), G2, and M (mitosis).
2) Upon completion of the M phase, the cell transforms into two cells, which immediately enter a new cycle in G1 (the possibility of temporary arrest in a G0 phase will be considered elsewhere).
3) Each phase is characterized by a mean duration D and a variability V. As soon as the prescribed duration of a given phase is reached, the transition to the next phase of the cell cycle occurs. The time at which the transition takes place varies in a random manner according to a distribution of durations of the cell cycle phases. In the case of a uniform probability distribution, the duration varies in the interval $[D(1-V), D(1+V)]$.
4) At each time step in each phase of the cycle the cell has a certain probability to be marked for exiting the cycle and dying at the nearest G1/S or G2/M transition. To allow for homeostasis, which corresponds to the maintenance of the total cell number in a range in which it oscillates, we further assume that cell death (with a probability of the order of 50% over 1 cycle) counterbalances cell replication at mitosis. When the probability of cell death is slightly smaller or larger than the value yielding homeostasis, the total number of cells increases or decreases in time, respectively.

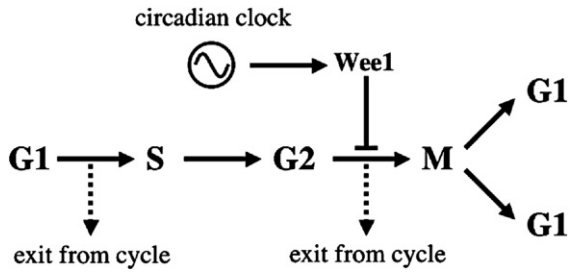

Fig. 2. Scheme of the automaton model for the cell cycle. The automaton switches sequentially between the phases G1, S, G2, and M after which the automaton cell divides and two cells enter a new G1 phase. Switching from one phase to the next one occurs in a random manner as soon as the end of the preceding phase is reached, according to a transition probability related to a duration distribution centered for each phase around a mean value D and a variability V (see text). Exit from the cell cycle occurs with a given probability at the G1/S and G2/M transitions. Coupling to the circadian clock occurs via the kinases Wee1 and cdc2 (Cdk1), which respectively inhibit and induce the G2/M transition.

In Table 1 of the Appendix we list the values assigned in the various figures illustrating the output of the modeling to the cell cycle length, presence or absence of cell cycle entrainment by the circadian clock, initial conditions, extent of cell phase variability and duration, and probability of quitting the cell cycle.

3. Dynamics of the cell cycle automaton in the absence or presence of entrainment by the circadian clock

The variability in the duration of the cell cycle phases is responsible for progressive cell desynchronization. In the absence of variability, if the duration of each phase is the same for all cells, the population behaves as a single cell. Then, if all cells start at the same point of the cell cycle, e.g., at the beginning of G1, a sequence of square waves bringing the cells synchronously through G1, S, G2, M, and back into G1 occurs (A. Altinok and A. Goldbeter, in preparation). The square waves will continue unabated over time. However, as soon as some degree of variability of the cell cycle phase durations is introduced, these square waves transform into oscillations through the cell cycle phases, the amplitude of which diminishes as the variability increases. In the long term, these oscillations dampen as the system settles into a steady state distribution of cell cycle phases: the cells are fully desynchronized and have forgotten the initial conditions in which they all started to evolve from the same point of the cell cycle (A. Altinok and A. Goldbeter, in preparation).

Shown in Fig. 3(A) is the oscillation in the fraction of cells in S phase, as a function of time, in the absence of entrainment by the circadian clock. In the case considered, the duration of the cell cycle is 22 h, and the variability V is equal to 5%. Because the variability is relatively low, cells do not tend to desynchronize much over time. However, if the variability were set to zero, no desynchronization would occur and the oscillations in the successive phases of the cell cycle would look like a succession of square waves. Conversely, when variability increases up to 15% in the absence of entrainment (Fig. 3(C)), the amplitude of the oscillations decreases, reflecting enhanced desynchronization.

Entrainment by the circadian clock can be included in the automaton model by considering that the protein WEE1 undergoes circadian variation due to induction by the complex between the circadian clock proteins CLOCK and BMAL1 of the expression of the *wee1* gene [3–5]. WEE1 is a kinase that phosphorylates and thereby inactivates the protein kinase cdc2 (also known as the cyclin-dependent kinase Cdk1) that controls the transition G2/M and, consequently, the onset of mitosis. In the mouse housed under a light–dark cycle of 12 h of light followed by 12 h of darkness (12:12 light–dark cycle), the WEE1 protein level rises during the second part of the dark phase, i.e., at the end of the activity phase. In general, human beings adhere to a routine of 16 h of diurnal activity alternating with 8 h of nocturnal sleep (see Fig. 3(B)); thus in the case of

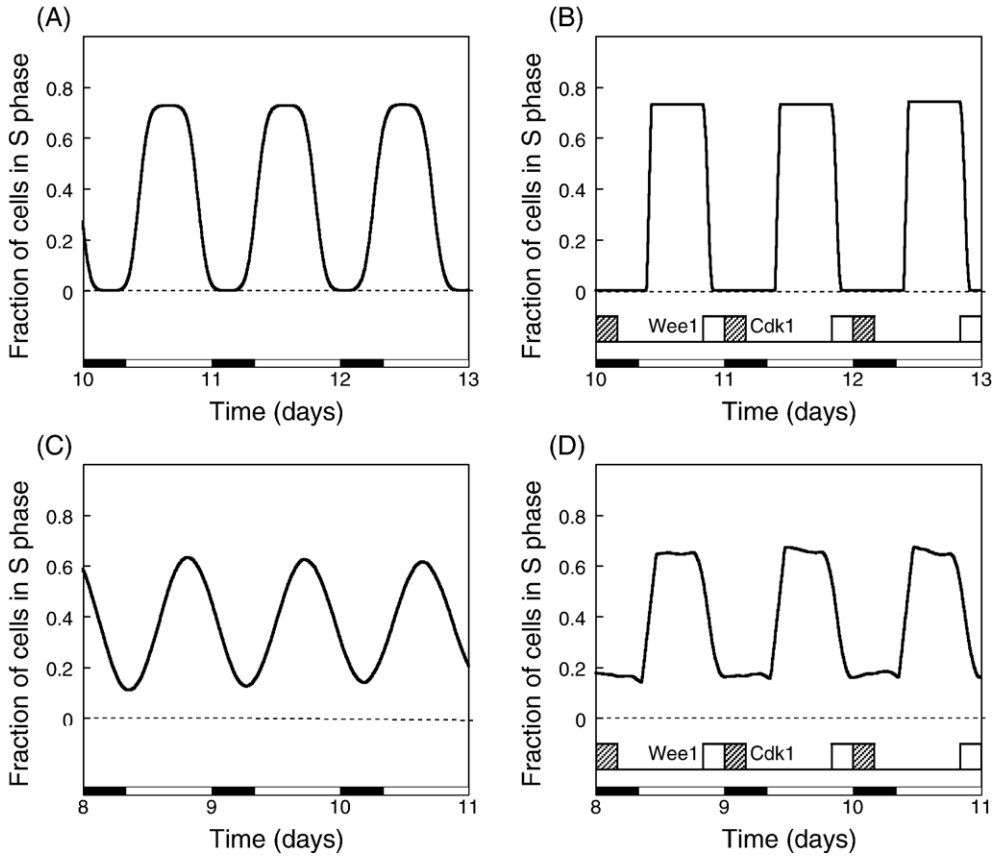

Fig. 3. Waves through cell cycle phases in absence (A, C) or presence (B, D) of entrainment by the circadian clock. The variability of durations for all cell cycle phases is equal to 5% (upper row) or 15% (bottom row). The curve, generated by numerical simulations of the cell cycle automaton model, shows the proportion of cells in S phase as a function of time, for days 10 to 13. The duration of the cell cycle before or in the absence of entrainment is 22 h. The successive phases of the cell cycle have the following mean durations: G1 (9 h), S (11 h), G2 (1 h), and M (1 h). As explained in Section 3, entrainment by the circadian clock occurs in the model via a 4-hour rise in Wee1 (from 8 p.m. to midnight) and a related, subsequent rise in Cdk1 (from midnight to 4 a.m.). The variations in Wee1 and Cdk1 are represented schematically in panels B and D below the curve showing the fraction of cells in S phase. The 24-hour light (L)–dark(D) cycle is shown as an alternation between an 8-hour long dark phase (black bar) and a 16-hour long light phase (white bar). Initial conditions are specified in Table 1 of the Appendix. The probability of quitting the cycle (in units of 10^{-3}/min) is equal to 0.5380 for A and C, 0.4925 for B, and 0.5150 for D; these values ensure homeostasis of the cell population, i.e., the number of cells in the population oscillates around and eventually reaches a stable steady state value.

human modeling, we will consider a 16:8 light–dark cycle (16 h of light, from 8 a.m. to 12 p.m., followed by 8 h of darkness, from 12 p.m. to 8 a.m.) [7,8,12,13]. The rise in WEE1 should occur at the end of the activity phase, i.e., from 8 to 12 p.m. The decline in WEE1 activity is followed by a rise in the activity of the kinase Cdk1, which enhances the probability of transition to the M phase. We shall consider that the 4-hour rise in WEE1 is immediately followed by a 4-hour rise in Cdk1 kinase. Thus, in the cell cycle model, the transition from G2 to M is blocked as soon as WEE1 rises, and the cell is held in G2 for 4 h, as long as the level of WEE1 is high. Conversely, we shall consider that every cell in G2 immediately passes into M as soon as the activity of Cdk1 is raised in a square wave manner.

Upon entrainment by the circadian clock, cells become more synchronized than in the absence of entrainment. In the case considered in Fig. 3(B) and (D), the period changes from 22 to 24 h, which corresponds to the period of the external LD cycle. When the variability is only of 5%, we observe that the fraction of cells in S phase goes to zero at the trough of the oscillations (Fig. 3(B)). This does not occur when the variability is higher, e.g., 15% (Fig. 3(D)). The fraction of the S-phase cells then oscillates with reduced amplitude, reflecting again the effect of desynchronization. In contrast to the progressive dampening of the oscillations in the absence of entrainment, oscillations appear to be sustained when the cell cycle automaton is driven by the circadian clock.

4. Assessing different patterns of circadian delivery of the anticancer drug 5-FU

4.1. Mode of action of 5-FU

S-phase cells exposed to 5-FU arrest in the S phase as a result of thymidilate synthase inhibition; then, they progress through the cell cycle or die through p53-dependent or independent apoptosis [11]. In the model we will consider that cells exposed to 5-FU while in the S phase have an enhanced probability of quitting the proliferative compartment at the next G2/M transition (Fig. 4(A)). The probability of quitting the cycle will be taken as proportional to the 5-FU concentration (Fig. 4(C)). We

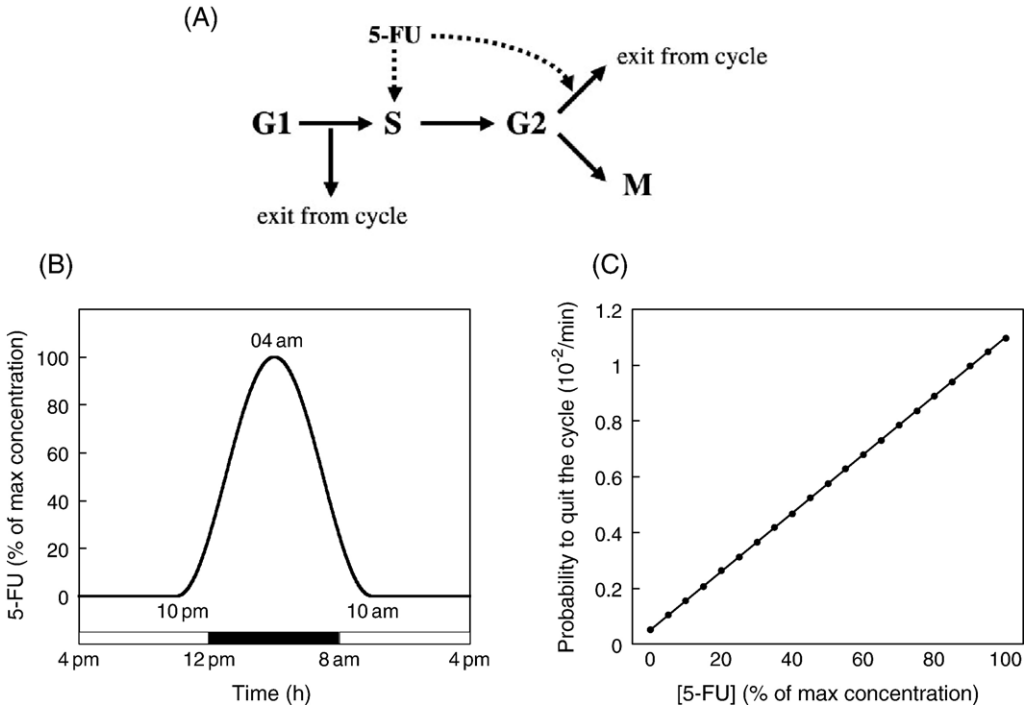

Fig. 4. (A) Scheme for action of 5-FU in the model. Cells exposed to 5-FU while in S phase have a higher probability of exiting the cell cycle at the next G2/M transition. (B) Semi-sinusoidal administration profile used clinically for 5-FU with peak time at 4 a.m. [27,28]. Over the 24-hour period, the 5-FU level is nil between 10 a.m. and 10 p.m., and rises in a semi-sinusoidal manner between 10 p.m. and 10 a.m. according to Eq. (1), with $A=100$ and $d=12$ h, with a peak at 4 a.m. (C) Probability of quitting the proliferative compartment as a function of 5-FU concentration, denoted [5-FU]. We assume that the probability p of exiting the cell cycle at the next G2/M transition after exposure to the drug during the S phase is proportional to [5-FU], according to Eq. (2). At the maximum of [5-FU] reached at 4 a.m., the basal value of the exit probability is thus multiplied by a factor of 21.

take a slope of the line such that the exit probability in the absence of 5-FU is multiplied by a factor close to 20 when the level of 5-FU reaches 100% of its maximum value. In the following we will consider that 5-FU varies in the range 0–100% in a semi-sinusoidal manner. Other hypotheses might be retained for the dose-response curve of the drug. Thus, larger or smaller slopes will respectively correspond to stronger or weaker cytotoxic effects of 5-FU. A threshold dependence may also be introduced, in which case the linear relationship must be replaced by a sigmoidal curve which tends to a step function as the steepness of the threshold increases.

In simulating the cell cycle automaton response to 5-FU, we will impose a circadian profile of the anticancer medication similar to that used in clinical oncology (Fig. 4(B)): 5-FU will be delivered in a semi-sinusoidal manner from 10 p.m. to 10 a.m., with a peak at 4 a.m. During the remaining hours of the day and night, the drug concentration will be set to zero. For comparison, we will consider similar drug-delivery patterns shifted in time, with peak delivery either at 10 a.m., 4 p.m., or 10 p.m.

The semi-sinusoidal delivery of the anticancer drug obeys the following equation which yields the concentration, [5-FU], as a function of time over the 24-hour -period:

$$[5\text{-FU}] = (A/2)[1 - \cos(2\pi(t - t_{\text{start}})/d)]. \quad (1)$$

For delivery over a period d starting at 10 p.m. and ending at 10 a.m. and with peak at 4 a.m., we take $t_{\text{start}}=22$ h and $d=12$ h, with $A=100$. The probability P of exiting the cell cycle after exposure to a given level of 5-FU during the S phase is given by Eq. (2):

$$P = P_0(1 + 0.2[5\text{-FU}]), \quad (2)$$

where P_0 is the basal probability to exit the cycle.

It will be useful to compare the circadian patterns of 5-FU delivery with the more conventional constant infusion drug-delivery pattern, in which the amount of 5-FU delivered over the 24-hour period is the same as for the circadian delivery schedules. The quantity of 5-FU ($Q_{5\text{FU}}$) delivered over 24 h according to the semi-sinusoidal schedule defined by Eq. (1) is given by Eq. (3):

$$Q_{5\text{FU}} = \int_0^d \frac{A}{2}\left(1 - \cos\left(\frac{2\Pi t}{d}\right)\right)dt = \frac{A}{2}(d + \sin 2\Pi - \sin 0) = \frac{A}{2}d. \quad (3)$$

For $A=100$ (in arbitrary concentration units (acu)) and $d=12$ h, this expression yields a mean 5-FU infusion rate of 5 acu/h.

4.2. Chronomodulated administration of 5-FU: effect of entrainment by the circadian clock

The effect of 5-FU on cell proliferation is illustrated in Fig. 5 in the absence (upper row) or presence (bottom row) of

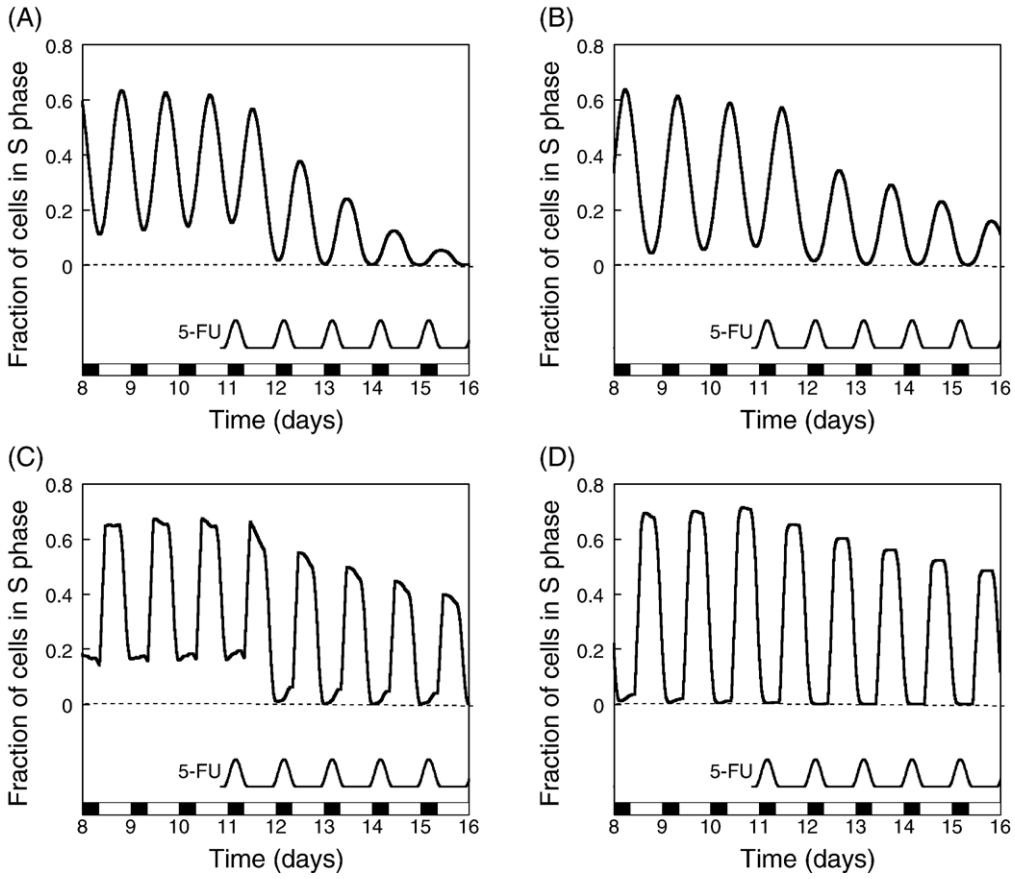

Fig. 5. Cytotoxic effect of 5-FU in the absence (upper row) or presence (bottom row) of entrainment of the cell cycle by the circadian clock, when the cell cycle duration is 22 (A and C) or 26 h (B and D), at a given variability V=15%. The curve shows the proportion of cells in S phase. Circadian administration of 5-FU begins at 10 p.m. on day 10 according to the semi-sinusoidal schedule shown in Fig. 4(B), and peaks at 4 a.m. Entrainment occurs in (C) and (D) as described in Fig. 3(B) and (D). Initial conditions and probabilities of exiting the cell cycle are specified in Table 1 of the Appendix.

entrainment by the circadian clock, for a cell cycle duration of 22 (left column) or 26 h (right column), i.e., for the cases where the cell cycle length without entrainment is shorter or longer than 24 h. To determine the effect of the circadian administration of 5-FU, we start periodic drug delivery after 10 days. The circadian schedule of 5-FU administration has a peak at 4 a.m. (see Fig. 4(B)), as used in clinical treatments. Shown in the four panels of Fig. 5 is the time evolution of the fraction of cells in S phase before and after 5 days of circadian drug delivery. The curve begins 8 days after the system commences its evolution from the set of initial conditions listed in the legend to Fig. 5.

We first note that in the absence of entrainment and before the beginning of 5-FU administration, the fraction of S-phase cells oscillates with decreasing amplitude. This behavior corresponds to the progressive desynchronization of the cell population. In the course of time, the amplitude of the oscillations will eventually decrease to zero and the fractions of cells in the four phases will reach steady state values. The time taken to reach the steady state shortens as the variability V increases (A. Altinok and A. Goldbeter, in preparation). Interestingly, although the same value of V was considered for panels A and B of Fig. 5, the amplitude of oscillations in the absence of entrainment is larger after the same number of days when the duration of the cell cycle is 26 h (panel B) as compared to 22 h (panel A), indicating that the progressive loss of synchronization is slowed in the former case. The reason is that cells which take more time to divide also take more time to undergo desynchronization.

As soon as 5-FU treatment begins, we observe a drop in the fraction of S-phase cells. However, because exit from the cell cycle occurs at the next G2/M transition for cells in S phase exposed to 5-FU (see Section 4.1 and Fig. 4(A)), the decrease in S-phase cells is delayed by one day with respect to the pattern of drug administration. This decline is largest for the response to the first pulse of 5-FU, and its amplitude decreases with the number of successive 5-FU pulses (see also Figs. 7 and 8 below). Panels C and D in Fig. 5 indicate that prior to 5-FU administration the cell cycle synchronizes to the circadian clock, both when the initial cell cycle duration is shorter or longer than 24 h. The amplitude of oscillations in the fraction of S-phase cells is larger than in the absence of entrainment, indicating enhanced synchronization. Moreover, the decline in S-phase cells in response to 5-FU is much reduced (compare panels C and D with A and B of Fig. 5, respectively). Entrainment of the cell cycle by the circadian clock thus strengthens cell synchronization and protects cells in S phase from the toxicity of 5-FU when the peak of 5-FU occurs at 4 a.m.

4.3. Circadian 5-FU administration: effect of variability of cell cycle phase durations

The cytotoxic effect of the circadian administration of 5-FU depends on a variety of factors including (a) the mean duration D of the cell cycle phases, (b) the variability V of cell cycle-phase durations, (c) entrainment by the circadian clock, and (d) timing of the daily peak in 5-FU. We already considered in Section 4.2 the effect of entrainment, and focus now on points (b) and (d). We will return in Section 4.4 to the effect of the timing of the circadian peak in 5-FU.

Shown in Fig. 6, as a function of variability V, is the cytotoxic effect of the 5-FU profile considered in Fig. 3(B), with the peak at 4 a.m., in the absence (panel A) and presence (panel B) of entrainment of the 22-hour cycle by the circadian clock. In both cases, the cumulated cell kill increases when V rises from 0 to

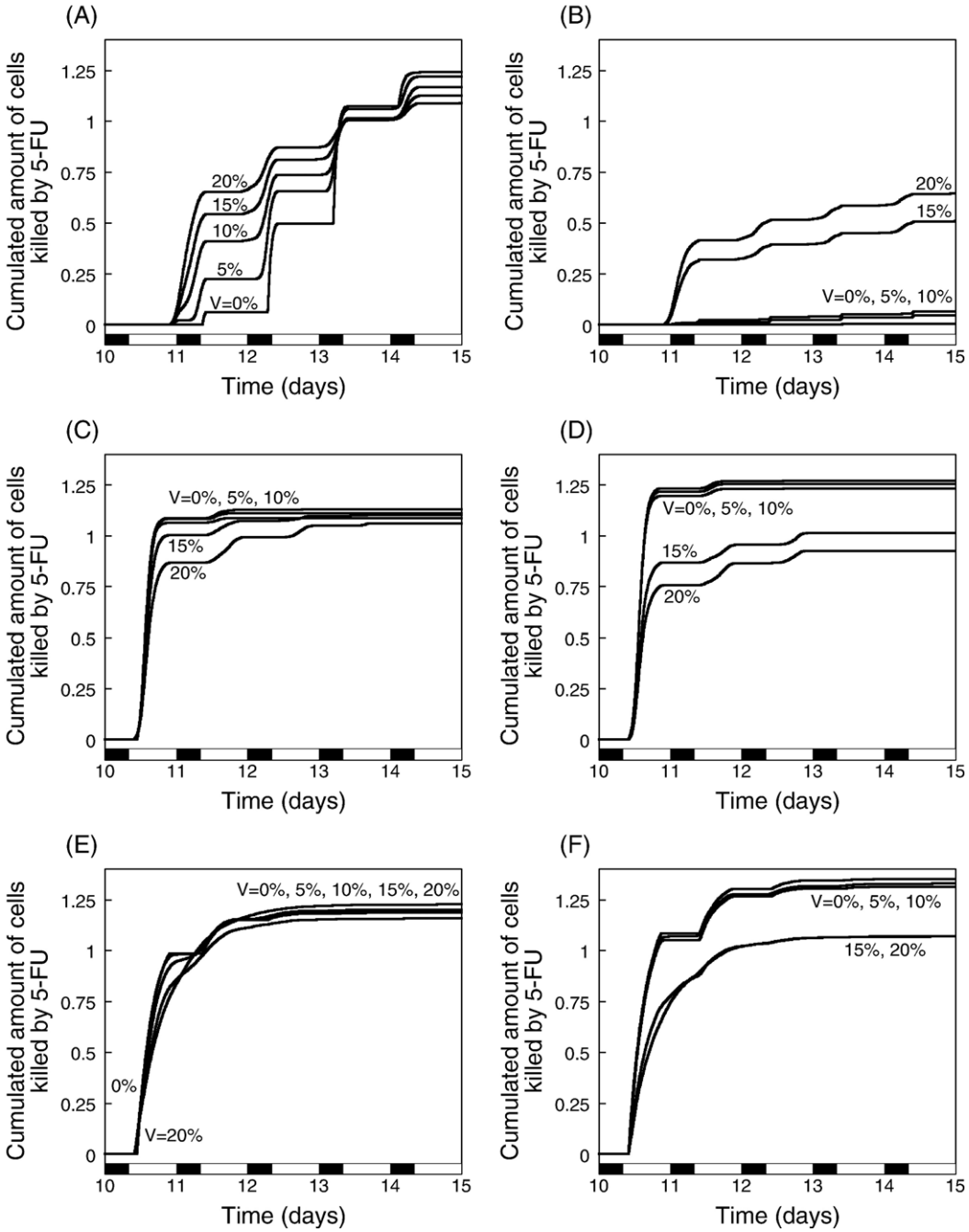

Fig. 6. Cytotoxicity of chronomodulated 5-FU: effect of variability of cell cycle phase durations. Shown is the cumulative cell kill (in units of 10^4 cells) when 5-FU is delivered in a circadian manner with peak at 4 a.m., in the absence (A, C, E) or presence (B, D, F) of entrainment by the circadian clock, for different values of variability V indicated on the curves. Panels in the upper and middle rows are established for a circadian delivery schedule peaking at 4 a.m. and 4 p.m., respectively. Panels E and F in the bottom row refer to a continuous infusion of 5-FU, which begins at 10 a.m. on day 10 (like the semi-sinusoidal infusion that peaks at 4 p.m.). Initial conditions and probabilities of exiting the cell cycle are specified in Table 1 of the Appendix.

20%. For this circadian schedule of 5-FU, which is the least toxic to the cells (see below), we see that the better the synchronization, the smaller the number of cells killed. In the presence of entrainment (Fig. 6(B)), a sharp increase occurs between $V \leq 10\%$ and $V \geq 15\%$ in the number of cells killed by the drug. This jump is not observed in the absence of entrainment (Fig. 6(A)). Thus, entrainment by the circadian clock further enhances the synchronization of cells and protects them from the drug, as long as V remains relatively small, i.e., $V \leq 10\%$. On the basis of Fig. 6(A) and (B), we may further conclude that entrainment by the circadian clock enhances the consequences of cell cycle variability, as it introduces a threshold in the effect of this parameter.

The effect of variability on drug cytotoxicity markedly depends on the temporal pattern of 5-FU delivery. This property is illustrated in Fig. 6(C) and (D), when the peak in the circadian delivery of 5-FU occurs at 4 p.m., by which the circadian schedule of 5-FU administration is most toxic to the cells (see below). Both in the absence (C) or presence (D) of entrainment by the circadian clock, cytotoxicity increases as the degree of variability decreases. The effect is more marked in the conditions of entrainment: a threshold in cytotoxicity then exists between $V = 10\%$ and 15% (Fig. 6(D)), although this threshold is less steep than in Fig. 6(B). For the circadian 5-FU delivery schedule with peak at 4 p.m, enhanced synchronization through decreased variability does not protect cells, but rather it increases their sensitivity to 5-FU cytotoxicity. We will further illustrate below the opposite effects of variability for the circadian delivery patterns of 5-FU with peak at 4 a.m. versus 4 p.m.

It is useful to compare the cytotoxic effects of 5-FU from its circadian patterning versus constant infusion. In panels E and F of Fig. 6 we show the results of simulations of the cell cycle automaton for constant 5-FU delivery, as a function of variability, in the absence and presence of entrainment by the circadian clock, respectively. The results closely resemble those obtained for the circadian patern with peak delivery at 4 p.m. (compare with panels C and D of Fig. 6). Cytotoxicity is comparable (see also Fig. 7(C) and (D) below), and a threshold is again observed in the case of entrainment, for a variability between 10% and 15%. As for the circadian pattern with peak at 4 p.m., cytotoxicity increases when synchronization is enhanced at low values of variability.

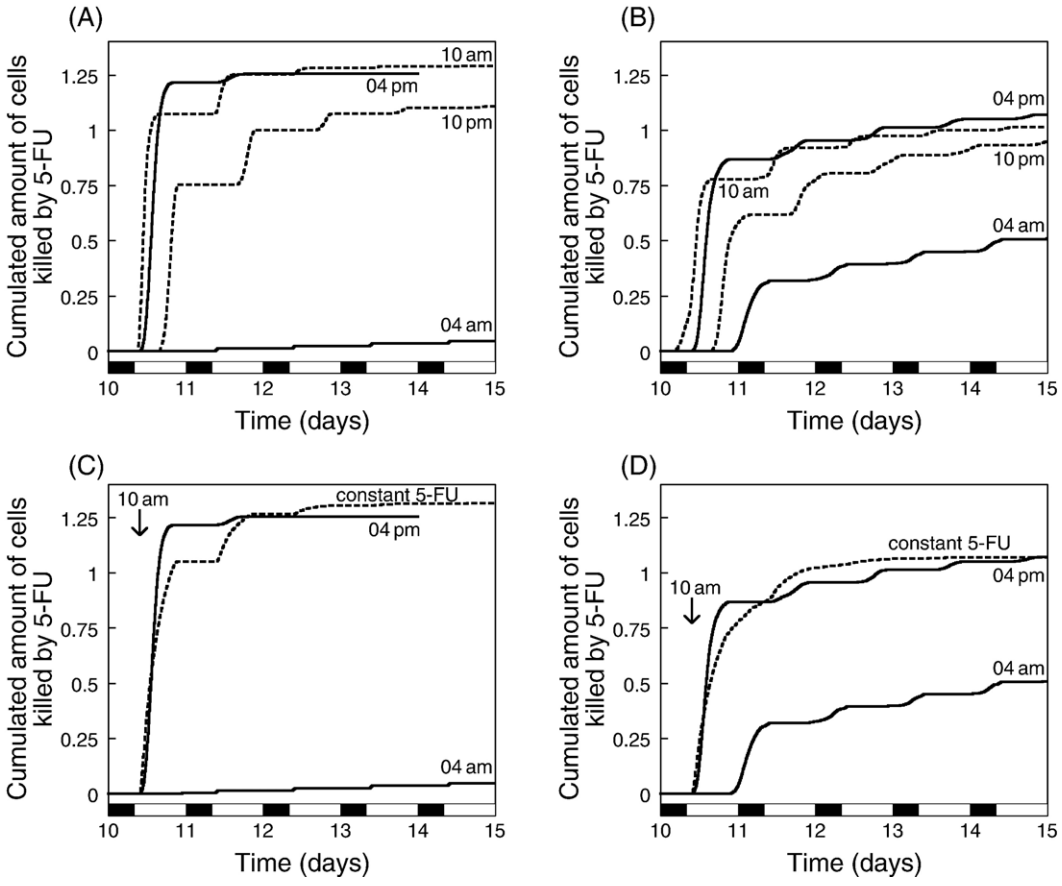

Fig. 7. Cytotoxicity of chronomodulated 5-FU: Effect of various circadian schedules of 5-FU delivery peaking at various times (4 a.m., 10 a.m., 4 p.m., 10 p.m.), when variability V is equal to 5% (A) or 15% (B). The circadian patterns peaking at 4 a.m. or 4 p.m. are compared in panels C ($V = 5\%$) and D ($V = 15\%$) with continuous delivery of 5-FU which begins at 10 a.m. on day 10 (vertical arrow) as in Fig. 6(F). The curves show the cumulated cell kill (in units of 10^4 cells) for days 10 to 15, in the presence of entrainment by the circadian clock. Prior to entrainment the cell cycle duration is 22 h. Parameter value and initial conditions are given in Table 1 of the Appendix.

4.4. Effect of circadian 5-FU schedule as a function of time of peak drug delivery

Turning to the effect of the peak time of circadian delivery of 5-FU, we now compare in the upper panels of Fig.7 four circadian schedules with peak delivery at 4 a.m., 10 a.m., 4 p.m., and 10 p.m., for a cell cycle variability of 5% (panel A) or 15% (panel B). The data on cumulated cell kill by 5-FU indicate a sharp difference between the circadian schedule with peak at 4 a.m., which is the least toxic, and the other schedules. This difference is more striking when cells are better synchronized (compare panels A and B). The most toxic circadian schedule is that with a peak delivery at 4 p.m. Then, indeed, all cells are killed after two pulses of 5-FU when cells are well synchronized (see also Fig. 8(C)): the curve is interrupted after four days of treatment. We compare in panels C and D of Fig. 7 the least and most toxic circadian patterns of 5-FU delivery with the continuous infusion of 5-FU. Continuous delivery of 5-FU appears to be nearly as toxic as the circadian pattern with peak at 4 p.m.

To clarify the reason why different circadian schedules of 5-FU delivery have distinct cytotoxic effects, we used the cell cycle automaton model to determine the time course of the fraction of cells in S phase in response to circadian drug administration in the two cases considered in Fig. 7, i.e., for a cell cycle variability of 5% (Fig. 8, panels A–D) or 15% (Fig. 8, panels E–H). The situation corresponds to Fig. 6B, namely, entrainment of a 22-hour cell cycle by the circadian clock. Let us first focus on the case where cells are well synchronized (V=5%). The data of panel A clearly indicate that the circadian schedule with peak at 4 a.m. is the least toxic. The reason is that the cells are well synchronized, with a circadian variation of the fraction of cells in S phase that is precisely in antiphase with the circadian profile of 5-FU. Thus, not only at the peak but during the whole phase of 5-FU administration does the fraction of cells in S phase remain close to zero. Since 5-FU only affects cells in the S phase, the circadian delivery of the anticancer drug in this case kills but a negligible amount of cells.

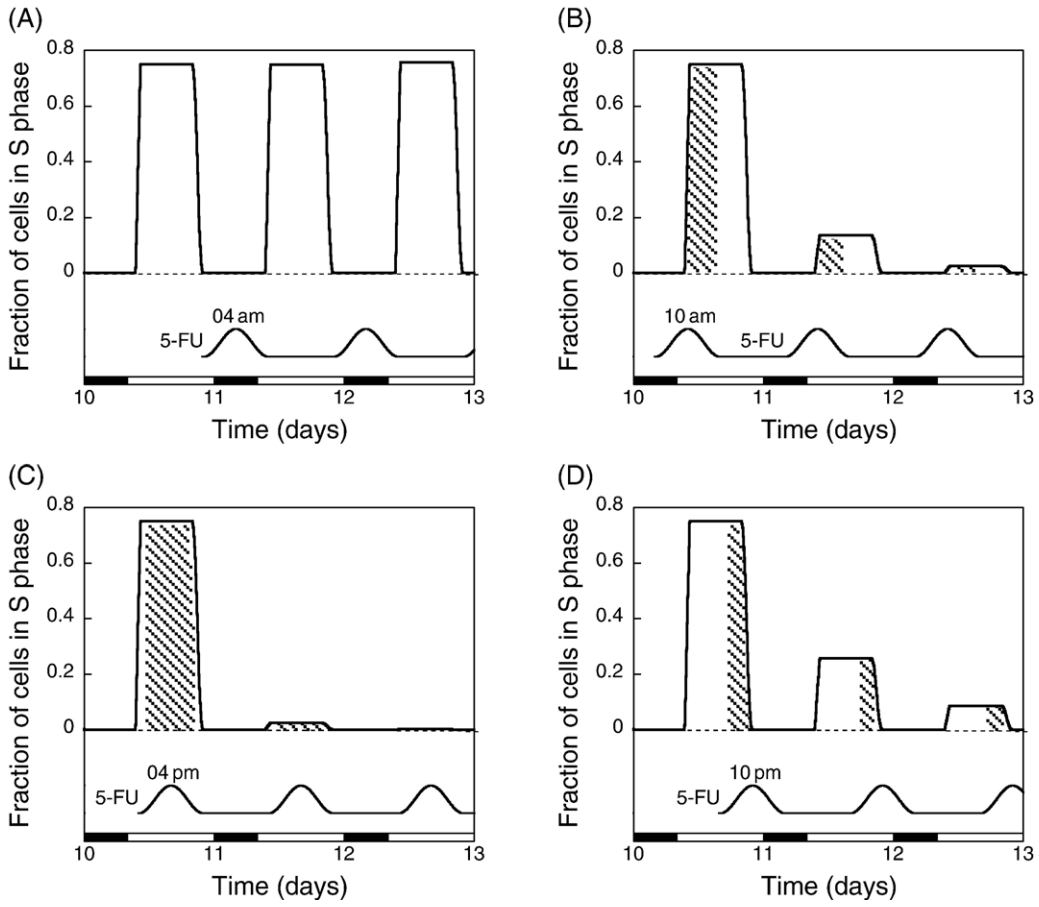

Fig. 8. Explanation of the cytotoxic effect of various circadian schedules of 5-FU delivery with peak at 4 a.m. (A, E), 10 a.m. (B, F), 4 p.m. (C, G), or 10 p.m. (D, H), and of continuous 5-FU delivery (I, J) for variability V=5% (A-D, I) and 15% (E-H, J). Data are obtained for a cell cycle duration of 22 h, in the presence of entrainment by the circadian clock. The hatched area shows the fraction of cells in S phase exposed to 5-FU and thus likely marked to exit the cell cycle at the next G2/M transition. The curves showing the cumulated number of cells killed (in units of 10^4 cells) indicate that the schedule with peak delivery at 4 a.m. is the one that causes minimal damage to the cells because the peak in 5-FU then coincides with the trough of the oscillations of S-phase cells. Continuous delivery of 5-FU is nearly as toxic as the most toxic circadian schedule of 5-FU delivery that peaks at 4 p.m., when variability is small (compare panels I and C). Because 5-FU is delivered at a constant, intermediate value in panels I and J, the probability of exiting the cell cycle is enhanced but not as much as at the peak of the semi-sinusoidal delivery illustrated in the other panels. Hatching marks are thus more spaced in I and J to indicate this effect. Parameter value and initial conditions are given in Table 1 of the Appendix.

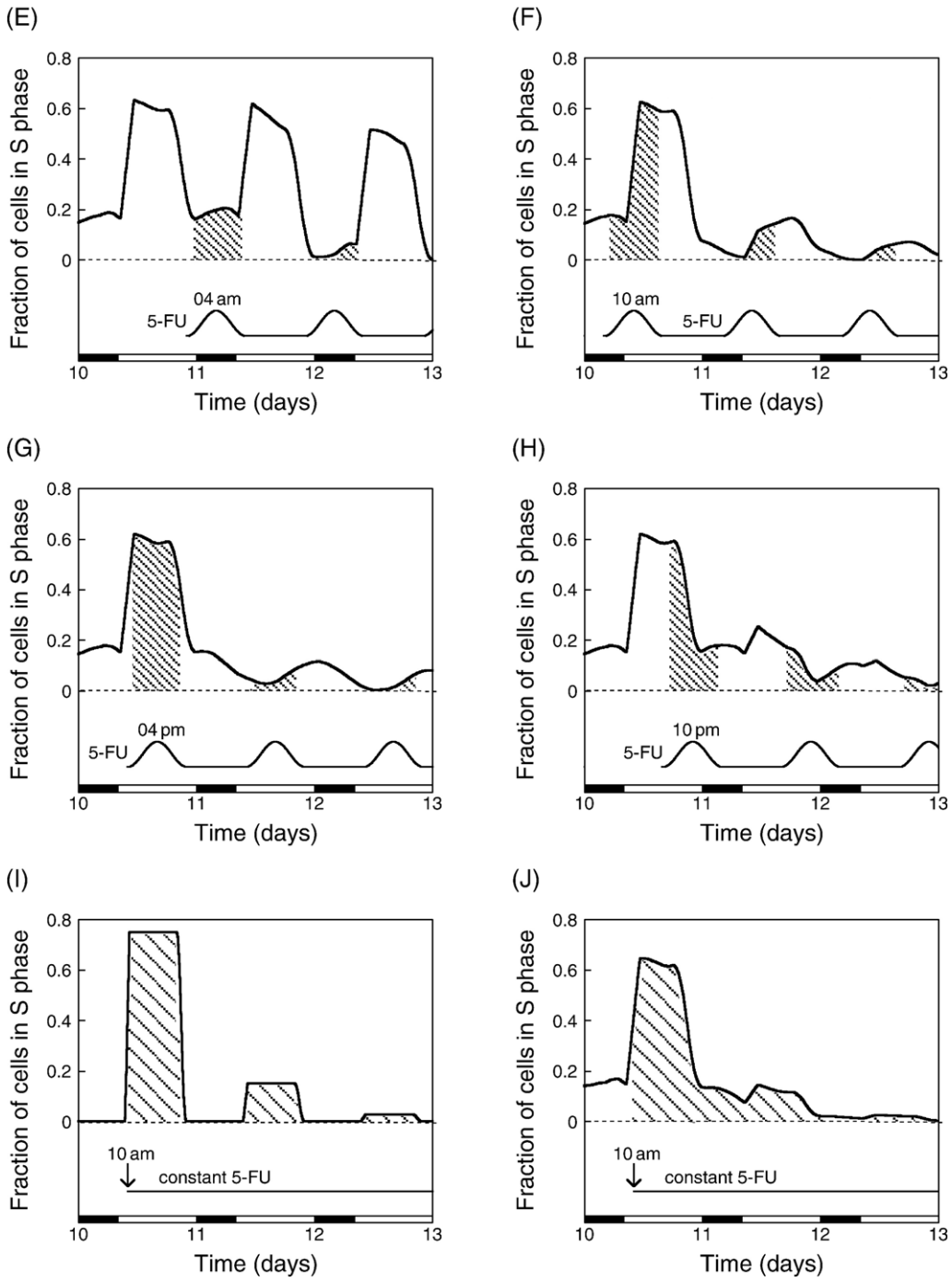

Fig 8. (*continued*).

When the peak delivery of 5-FU is at 4 p.m., the situation is opposite: now, the phase of 5-FU administration precisely coincides with the time period during which cells pass in a quasi-synchronous manner through the S phase (Fig. 8(C)). As a result, the first peak in S-phase cells is nearly annihilated following drug exposure. The remaining cells will die after exposure to the second 5-FU pulse, which again coincides with the next peak of S-phase cells. The latter peak is much smaller than the first one, because most cells exited the cycle after exposure to the first 5-FU pulse.

The cases of peak delivery at 10 a.m. (Fig. 8(B)) or 10 p.m. (Fig. 8(D)) are intermediary between the two preceding cases. Overlap between the peak of 5-FU and the peak of cells in S phase is only partial, but it is still greater in the case of the peak at 10 a.m., so that this pattern is the second most toxic, followed by the circadian delivery centered around 10 p.m. The comparison of the four panels A–D explains the results of Fig. 7(A) on the marked differences in cytotoxic effects of the four 5-FU circadian delivery schedules. The use of the cell cycle automaton helps clarify the dynamic bases that underlie the distinctive

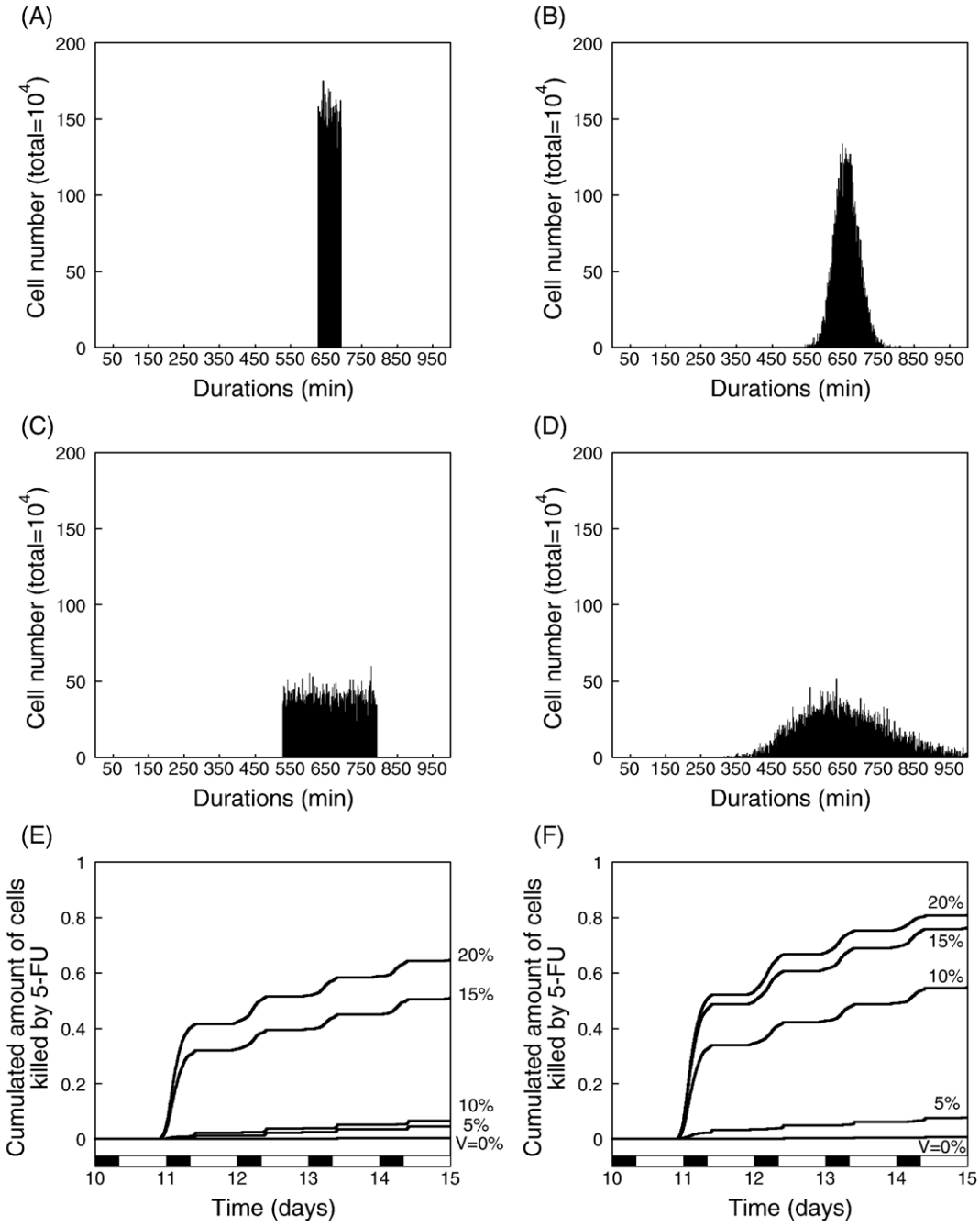

Fig. 9. Comparison of cumulative cell kill (in units of 10^4 cells) by 5-FU for the uniform (E) and lognormal distributions (F) of durations of cell cycle phases. The circadian pattern of 5-FU delivery peaks at 4 a.m. Data are obtained for a cell cycle duration of 22 h, in the presence of entrainment by the circadian clock, for increasing values of the variability *V*. The uniform and lognormal distributions [Eq. (4)] of durations of the S phase (mean duration: 11 h) are shown in the upper and middle rows on the left and right, respectively, for $V=5\%$ (A) or 20% (C), and $\sigma=5\%$ (B) or 20% (D).

effects of the peak time in the circadian pattern of anticancer drug delivery.

When cells are less synchronized, e.g., in the presence of entrainment by the circadian clock for a variability of 15%, the results are similar; although, the cytotoxic effect of the drug is reduced. Thus, for a peak delivery of 5-FU at 4 a.m., drug delivery is still in antiphase with the oscillation in the S-phase cells (Fig. 8(E)), but because the cells are less synchronized the fraction of S cells does not goes to zero at its trough, as it did for $V=5\%$ (Fig. 8(A)). As a result, some cells remain in S phase during the 5-FU pulse, so that a cytotoxic effect is observed. However, the fraction of S-phase cells does approach zero at the next trough. In consequence, only a few additional cells are killed by the second 5-FU pulse. For the pattern with peak drug delivery at 4 p.m. (Fig. 8(G)), the situation is again close to the case of panel C: the peak of 5-FU precisely overlaps with the peak of cells in S phase, but because cells are less synchronized the amplitude of the peak in S cells is smaller. The amount of cells killed after the

first 5-FU pulse is thus large, but relatively smaller than in the case when cells are better synchronized. Here again most cells killed by 5-FU exit the cycle after the first pulse of the drug. Panels F and H show that partial overlap of the drug pulse with the peak of cells in S phase yields relative cytotoxic effects which account for the differences in cumulated cell kill shown in Fig. 7(B).

The case of the continuous infusion of 5-FU is considered in panels I (V=5%) and J (V=15%) of Fig. 8. Because the total amount of 5-FU administered over the 24 h is the same as for the circadian semi-sinusoidal patterns, the level of 5-FU – and hence the cytotoxic effect of the drug – is sometimes below and sometimes above that reached with the circadian schedule. The numerical simulations of the automaton model indicate that the cytoxicity is slightly less than that observed for the most toxic circadian pattern, with peak delivery of 5-FU at 4 p.m. (compare panels I and J with panels C and G, respectively, of Fig. 8).

The data of Figs. 7 and 8 lead us to conclude that the least damage to the cells occurs when the peak of 5-FU circadian delivery is at 4 a.m., and when cells are well synchronized, i.e., when cell cycle variability V is lowest. In contrast, when the peak of 5-FU circadian delivery is at 4 p.m., cytotoxicity is enhanced when cells are well synchronized. The cytotoxic effect of the drug, therefore, can be enhanced or diminished by increased cell synchronization, depending on the relative phases of the circadian schedule of drug delivery and of the cell cycle entrained by the circadian clock. Continuous infusion of 5-FU is nearly as toxic as the most cytotoxic circadian pattern of anticancer drug delivery.

4.5. Uniform versus lognormal distribution of cell cycle phase durations

All the above results have been obtained for the case where the durations of the various cell cycle phases obey a probability distribution centered around the mean duration D, with a range of variation extending uniformly from $D-V$ to $D+V$. The uniform probability distribution generated by numerical simulations of the automaton for an S phase having a mean duration of 11 h (660 min) is shown in Fig. 9(A) and (C), when variability is 5% and 20%, respectively. Shown in Fig. 9(B) and (D) are the corresponding results for the probability distribution, when assuming a lognormal distribution centered around the same mean value, with a standard deviation of 5% and 20%, respectively.

The lognormal distribution obeys Eq. (4):

$$f(x) = \frac{1}{\sqrt{2\Pi}\sigma x} \exp\left(-\frac{\ln x - \mu}{\sigma}\right)^2 \quad (4)$$

where μ denotes the mean value of the phase duration x, and σ^2 the variance.

The results on cell kill by 5-FU depend in a certain measure on the type of probability distribution taken for the durations of the cell cycle phases. We compare in Fig. 9(E) and (F) the cytotoxic effect of 5-FU delivered in a circadian schedule with peak administration at 4 a.m., when the durations of the various cell cycle phases obey a uniform (panel E, identical to Fig. 6(B)) or lognormal distribution (panel F). The fact that the lognormal distribution extends over a more extended range results in a reduced degree of synchronization. Consequently, although this circadian pattern of 5-FU delivery is the least toxic (see Figs. 7 and 8), more S-phase cells are exposed to 5-FU, and thus the drug cytotoxicity is enhanced. The data of Fig. 9(F), nevertheless, indicate that a threshold in the variability also exists for the lognormal distribution, and that the effect of variability is qualitatively similar to that obtained in Fig. 9(E) for the uniform distribution.

5. Discussion

Circadian rhythms in human beings govern a large number of physiological functions, including the sleep–wake cycle and nutrition. Moreover, many hormone levels and enzyme activities display circadian patterns. Circadian rhythms, accordingly, play important roles in both health and disease. Clinical work aims at taking into account the therapeutic implications of circadian rhythms. Determining the appropriate biological time to administer medications to maximize their efficacy and/or minimize unwanted toxicity and other side-effects is the main goal of research involving the chronopharmacology and chronotherapeutics of medications. The chronotherapeutic approach is currenty being tested thoroughly in cancer. The study of various anticancer drugs shows that each possesses an optimal circadian delivery pattern, according to the phase of the cell cycle in which the cytotoxic effect is exerted. At the present time, programmable pumps are used for the concomitant administration of several anticancer drugs, each of which can be chronomodulated in a circadian manner according to a specific temporal pattern [10–14]. The findings of these clinical studies document the merit of cancer chronotherapy, and they also serve as the basis for the development in the future of tablet cancer chronotherapies.

The chronopharmacological properties of anticancer drugs were first established in studies on rodents, before being extended to humans. An important difference between the two species is that rodents are nocturnal animals in contrast to humans who possess an opposite, diurnal pattern of activity. As a consequence, many anticancer drugs that are more efficient on tumor cells or less toxic to healthy tissues at night or during the daytime in rodents will have similar properties during the corresponding phase of the human rest-activity cycle and thus will be shifted by roughly 12 h with respect to the 24 h period [6,10–14]. A case in point is provided by 5-Fluorouracil (5-FU). This widely used anticancer drug interferes with DNA synthesis and acts during the DNA replication, S phase, of the cell cycle. Cells exposed to 5-FU during the S phase have an enhanced probability of dying from apoptosis at the next G2/M transition. In rodents, the cytotoxicity of the drug is much stronger when it is delivered under continuous infusion or in a circadian pattern with maximum delivery at 4 a.m. Minimum cytotoxicity is observed for a circadian pattern with peak delivery at 4 p.m. In humans, the result is opposite: the circadian patterns of 5-FU administration with peak delivery at 4 a.m. and 4 p.m. are, respectively, the least and most cytotoxic. In addition, for reasons which are still unclear, maximum 5-FU cytotoxicity to tumor cells occurs at the same time as best 5-FU tolerance,

i.e., minimal damage to healthy tissues. In anticancer treatment, 5-FU is therefore administered according to a semi-sinusoidal pattern with peak delivery at 4 a.m. [27,28].

It would be useful to base these empirical results on the effect exerted by the anticancer drug on the cell cycle in tumor and normal cells. This would not only help explain the dependence of cytotoxicity and tolerance on the temporal pattern of drug administration, but it would also provide firm foundations at the cellular level for the chronotherapeutical approach. Studies of the cell cycle have recently brought to light a direct link with the circadian clock. The protein complex CLOCK-BMAL1, which plays a central role in the molecular mechanism of the mammalian circadian clock, indeed induces the periodic expression of the *wee1* gene [3–5]. Since the protein kinase Wee1 inhibits the kinase cdc2 (also known as Cdk1), which itself triggers the G2/M transition, induction of WEE1 by CLOCK-BMAL1 provides a direct link of the cell cycle to the circadian clock. This mechanism directly bears on the enhanced efficiency of the circadian administration of anticancer medications, such as 5-FU. Other links between the circadian clock and cancer exist. Thus, mice bearing mutations of the circadian clock protein Per2 have a higher propensity of developing spontaneous tumors [1]. Moreover, mice whose suprachiasmatic nuclei (the master pacemaker circadian clock) have been suppressed, and which therefore lack the central pacemaker generating circadian rhythms, also display an increased rate of tumor progression [2]. The link between circadian rhythms and cancer, therefore, bears both on the rate or propensity of tumor progression and on the cytotoxicity of anticancer drugs.

To investigate the link between the cell cycle and the circadian clock and to assess the effect of circadian patterns of anticancer drug delivery, it is useful to complement experimental studies by a modeling approach. Computational models allow a rapid exploration of a molecular or cellular mechanism over a wide range of conditions [15,16]. What is needed is thus a model for the cell cycle, allowing the study of its coupling to the circadian clock and of the effect of cytotoxic drugs. Rather than resorting to a detailed molecular model for the cell cycle in terms of cyclins and cyclin-dependent kinases and their control — models of this sort are available [16–19] and are currently being extended (C. Gérard and A. Goldbeter, manuscript in preparation), we used here a phenomenological approach in which the progression between the successive phases of the cell cycle is described by a stochastic automaton. This model is closely related to an automaton model previously proposed for the growth of human hair follicles [23,24]. Here, the cell

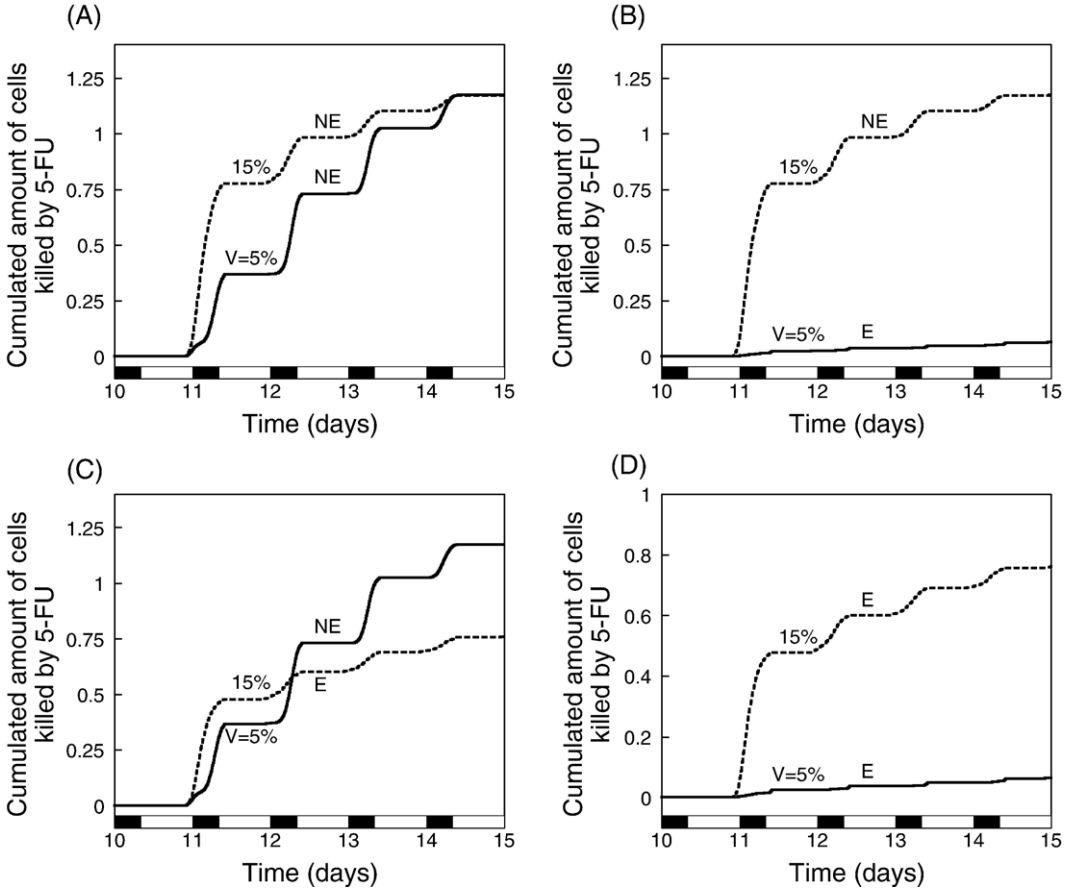

Fig. 10. Comparison of cumulative cell kill (in units of 10^4 cells) by circadian delivery of 5-FU with a peak at 4 a.m. for two cell populations differing by variability *V*, equal to 5% for population 1 and 15% for population 2. (A) None of the two populations is entrained by the circadian clock (NE = not entrained); (B) only population 1 is entrained (E = entrained); (C) only population 2 is entrained; (D) both populations are entrained by the circadian clock. The two cell populations have the same cell cycle duration of 22 h in the absence of entrainment (see Table 1 of the Appendix for parameter values and initial conditions).

cycle automaton switches sequentially between the phases G1, S, G2, and M, with a probability related to the duration of the various cell cycle phases. Each phase is characterized by its mean duration *D* and by its variability *V*. Upon mitosis (phase M), cells divide and enter a new cycle in G1. Exit from the cell cycle, reflecting cell death, occurs at the G1/S and G2/M transitions. Appropriate values of the exit probability allow for homeostasis of the total cell population. The anticancer drug 5-FU augments the exit probability for those cells that have been exposed to 5-FU during the S phase of DNA replication. An advantage of the stochastic automaton model is that it can readily be simulated to probe the cytotoxic effect of various circadian or continuous patterns of anticancer drug delivery.

The model shows that when all cells commence at the same phase, e.g., G1, for cells that are initially synchronized, they can either remain synchronized in the course of time, or they progressively become desynchronized. Desynchronization occurs when the durations of the cell cycle phases are distributed around a mean value with a certain variability. The greater the variability, the sooner cells will desynchronize until, eventually, a steady state distribution of cells between the various cell cycle phases will be established. On the way to steady state, cells will undergo oscillations in the fractions of cells in the G1, S, G2, and M phases, associated with wavelike transitions between the successive phases of the cell cycle. These basic properties of the cell cycle automaton model will be reported in detail elsewhere (A. Altinok and A. Goldbeter, in preparation).

The waveform of the oscillations has the appearance of a square wave in the case of zero variability, i.e., cells then remain synchronized. These square-wave oscillations transform into smoother oscillations of smaller and smaller amplitude as variability progressively increases. We showed that the cell cycle automaton model can be entrained by the circadian clock when incorporating a circadian block of the transition between the G2 and M phases, reflecting the circadian increase in the kinase Wee1. This increase takes place at the time set by the rise of the circadian clock protein BMAL1 in humans. Likewise, we incorporated the effect of the circadian increase in the kinase Cdk1, which immediately follows the peak in Wee1. The effect of Cdk1 corresponds in the model to an enhanced probability of transition between the G2 and M phases. Coupling the cell cycle automaton to the circadian variation of Wee1 and Cdk1 thus permits the entrainment of the cell cycle by the circadian clock, at a

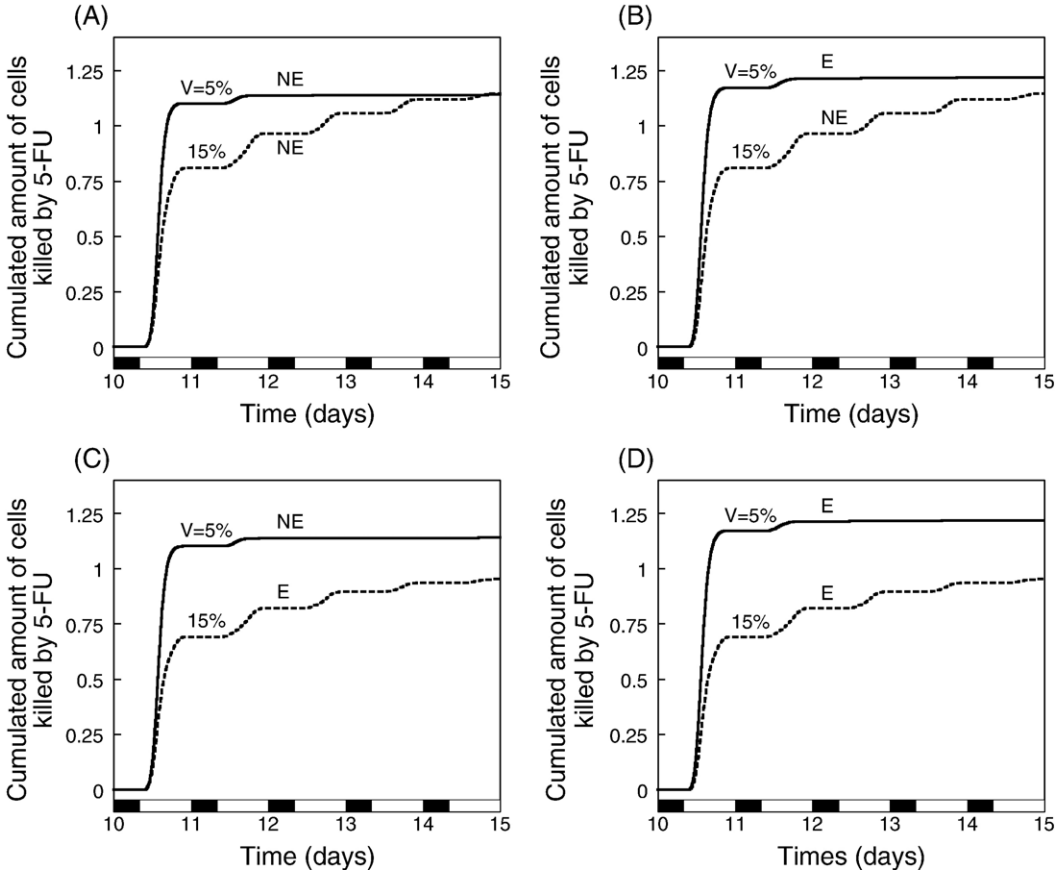

Fig. 11. Comparison of cumulative cell kill (in units of 10^4 cells) by circadian delivery of 5-FU with a peak at 4 p.m. for two cell populations differing by variability *V*, equal to 5% for population 1 and 15% for population 2. (A) None of the two populations is entrained by the circadian clock; (B) only population 1 is entrained; (C) only population 2 is entrained; (D) both populations are entrained by the circadian clock. The two cell populations have the same cell cycle duration of 22 h in the absence of entrainment. Parameter values and initial conditions are given in Table 1 of the Appendix.

phase that is set by the timing of the peak of the circadian clock protein BMAL1. Entrainment strengthens cell synchronization (Fig. 5). The peak of cells in S phase is of particular relevance for the action of 5-FU. The model predicts, upon entrainment by the circadian clock, that in human beings the greatest (peak) fraction of cells in S phase occurs during the light phase, around 4 p.m., and that the lowest (minimum) fraction occurs during the night, around 4 a.m. (Fig. 3(B) and (D)).

Measuring the cytotoxic effect of the drug by the normalized, cumulated number of cells killed by 5-FU, we compared the effect of the continuous administration of 5-FU with various circadian patterns of 5-FU delivery peaking at 4 a.m., 10 a.m., 4 p.m., or 10 p.m., in the absence or presence of entrainment by the circadian clock (Figs. 6 and 7). Several conclusions can be drawn from this comparison. First, the various circadian patterns of 5-FU delivery have markedly different cytotoxic effects on diurnally active cancer patients: the least toxic pattern is that which peaks at 4 a.m., while the most toxic one is that which peaks at 4 p.m. The other two patterns peaking at 10 a.m. or 10 p.m. exert intermediate cytotoxic effects. Conventional continuous infusion of 5-FU is nearly as toxic as the circadian pattern of 5-FU delivery peaking at 4 p.m.

The cell cycle automaton model permits us to clarify the reason why circadian delivery of 5-FU is least or most toxic when it peaks at 4 a.m. or 4 p.m., respectively. Indeed, the model allows us to determine the relative positions of the peaks in S-phase cells and in 5-FU. As shown in Fig. 8, 5-FU is least cytotoxic when the fraction of S-phase cells (peak at 4 p.m. and trough near 4 a.m.) oscillates in antiphase with 5-FU (peak at 4 a.m.) and most toxic when both oscillate in phase (peak of 5-FU at 4 p.m). Intermediate cytotoxicity is observed for the other circadian patterns of 5-FU (peak at 10 a.m. or 10 p.m.), for which the peak of 5-FU partially overlaps with the peak of S-phase cells. For the continuous infusion of 5-FU, the peak in S-phase cells necessarily occurs in the presence of a constant amount of 5-FU. Hence, the constant delivery pattern is nearly as toxic as the circadian pattern peaking at 4 p.m.

The goal of anticancer chronotherapies is to maximize the cytotoxic effect of medications on the tumor while protecting healthy tissues to achieve enhanced patient tolerance. The question arises as to how the above results might be used to predict the differential effect of an anticancer drug such as 5-FU on normal and tumor cell populations. This issue relates to the ways in which normal and tumor cells differ [29]. Such differences may pertain to the characteristics of the cell cycle, e.g., duration of the cell cycle phases and their variability, or entrainment of the cell cycle by the circadian clock. For the sake of clarity, let us focus on the case of two cell populations, one which corresponds to tumor and the other to healthy tissue. Let us assume that the two cell populations have the same durations of the cell cycle phases, but differ by the variability which is equal to 5% (population 1 of healthy cells) or 15% (population 2 of tumor cells). We will compare the effect of two circadian patterns of 5-FU delivery, with peak at 4 a.m. or 4 p.m., when none of the two populations is entrained by the circadian clock, when only population 1 or population 2 is entrained, or when both populations are entrained.

The results shown in Fig. 10 indicate that when the circadian delivery of 5-FU peaks at 4 a.m. the differential effect of the drug on the two cell populations is largest when population 1 ($V=5\%$) is entrained by the circadian clock, whether population 2 ($V=15\%$) is (panel D) or is not (panel B) entrained. In both cases, the cytotoxic effect of 5-FU on tumor cells, characterized by the largest variability, is much stronger. A similar observation can be made when none of the two populations is entrained by the circadian clock (panel A) or when population 2 but not population 1 is entrained (panel C). In these cases, however, the differential effect of 5-FU on the two cell populations is not as significant as in the two previous cases. Thus, as previously noted, synchronization of the cells minimizes cytotoxic damage when the circadian 5-FU modulated delivery pattern peaks at 4 a.m.

As illustrated in Fig. 11 the results are markedly different when the circadian pattern of 5-FU delivery peaks at 4 p.m. The differential effect of 5-FU is again largest when population 1 with lowest variability is entrained by the circadian clock, whether population 2 with largest variability is entrained (panel D) or not (panel B). Now, however, the cytotoxic effect is most detrimental to population 1, and the difference between the two populations is not as strong as that shown in the corresponding panels of Fig. 10. Again, this is the case, though to a milder degree, when none of the two populations is entrained (panel A) or when only population 2 is entrained (panel C). We see that when 5-FU delivery peaks at 4 p.m. the cytotoxic effect of the drug on the two populations is the inverse as that predicted for the circadian pattern peaking at 4 a.m. (compare Figs. 10 and 11). The effect of variability thus depends on the circadian pattern of 5-FU delivery and on the possibility of entrainment of the cell cycle by the circadian clock.

The results presented here point to the interest of measuring, both in normal and tumor cell populations, parameters such as the duration of the cell cycle phases and their variability, as well as the presence or absence of entrainment by the circadian clock. As shown by the results obtained with the cell cycle automaton model, these data will be crucial for using the model to predict the differential outcome of various anticancer drug delivery schedules on normal and tumor cell populations. In a second step, we plan to incorporate the pharmacokinetic-pharmacodynamic (PK-PD) aspects of 5-FU metabolism into the modeling approach. The, enzymes involved in the degradation and utilization of 5-FU follow inverse circadian activity patterns [26]. For 5-FU, however, these variations might not be highly significant, because the half-life of 5-FU is relatively brief with respect to the circadian timescale [25].

The results presented here show that the cell cycle automaton model displays a high sensitivity to the rate of spontaneous exit from the cell cycle. Progressive explosion or extinction of the cell population occurs for a value of the exit rate slightly below or above the value yielding homeostasis, i.e., stabilization of the cell count which oscillates in a constant range without displaying any oscillatory exponential increase or decrease. This result stresses the physiological importance of this parameter, which is likely controlled by the cell population as a function of total cell mass. Such an auto-regulation might obviate the need to

specify with great accuracy the cell cycle exit rate to guarantee homeostasis.

The present modeling approach to circadian cancer chronotherapy is based on an automaton model for the cell cycle. Continuous approaches to cell cycle progression have also been used to study the link between cell proliferation and circadian rhythms [30] and to determine, in conjunction with optimal control theory, the most efficient circadian schedules of anticancer drug administration [31].

Besides circadian cancer chronotherapy, another line of research resorting to periodic schedules of anticancer drug delivery has been proposed [32–35]. It is based on a resonance phenomenon between the period of drug administration and the cell cycle time of the normal tissue. The goal of this approach is again to develop a strategy that limits, as much as possible, damage to the normal sensitive tissue, while maximizing the destruction of tumor cells. While the assessment of circadian cancer chronotherapy has for long been the topic of multi-center clinical studies, the approach based on resonance in periodic chemotherapy has largely remained a topic of interest to theoreticians, supported so far by a limited number of experimental studies [36,37], but yet to be tested clinically. The main idea behind the latter approach is that the periodic scheduling of phase-specific cytotoxic agents can increase the selectivity of therapy when the treatment period is close to the mean cycle length of proliferation of normal susceptible cells, provided the cell cycle time of normal cells differs from that of malignant cells. A first dose of chemotherapy will kill all cells if it coincides in time to the sensitive phase of the cell cycle; these cells will not produce any daughter cells. If the next dose is administered at a time when these daughter cells would have been susceptible to chemotherapy, cells at other phases of the cell cycle will be protected. Damage to the population of normal cells should thus remain limited when chemotherapy is administered with a period close to the normal cell cycle time. In contrast, each dose of chemotherapy should kill another fraction of the tumor cell population because the latter cells divide with a different periodicity.

Dibrov and Agur and their colleagues [32–37] presented a theoretical treatment of the resonance effect as well as experimental data in mice to support the theoretical conclusions. The phenomenon of resonance in periodic chemotherapy has been analyzed further in more refined cell population models [38]. Clinical studies based on the resonance effect are still lacking, however. Potential difficulties inherent in this approach were examined by means of a theoretical model of acute myelogenous leukemia [39]. Based on estimates of cell cycle parameters, and on a model for the cell cycle kinetics of normal bone marrow and malignant cells, the authors concluded that chronotherapy based on the resonance effect is unlikely to be efficacious in the treatment of this particular disease. One reason is feedback: the treatment, itself, may alter the kinetic parameters characterizing the tumor in such a way that the average intermitotic interval varies in the course of chemotherapy. The resonance-based efficiency of chronotherapy might wane if the difference of cell cycle length between normal and malignant cells declines as a result of drug administration.

In trying to distinguish circadian chronotherapy from resonance chronotherapy, we should point not only to differences but also to similarities. The present study stresses the effect of variability, which can enhance the differential cytotoxic effect of the anticancer drug on the normal and tumor cell populations. Moreover, resonance chronotherapy relies on a difference between cell cycle durations in the two populations, which is not required in the case of cancer circadian chronotherapy. Nevertheless, the idea of resonance is also present in the case of circadian 5-FU delivery. Indeed, the circadian patterns of 5-FU which peaks at 4 a.m. or 4 p.m. correspond to oscillations that are, respectively, in antiphase or in corresponding phase with the circadian variation of the fraction of cells in S-phase. This effect can be seen even for cell cycle durations that differ from 24 h, because of the entrainment of the cell cycle by the circadian clock.

In the field of cancer chronotherapy, two lines of research pertain to the search for optimal patterns of drug administration. The approach based on a resonance phenomenon in periodic chemotherapy has been primarily studied from a theoretical point of view. Although supported by experiments performed on laboratory mice, it has not been tested yet in a clinical setting. The alternative approach, based on circadian chemotherapy, has been tested in experiments with laboratory rodents and its clinical evaluation is still in progress, involving multi-center clinical studies on cancer patients [12].

We used the cell cycle automaton model to probe the cytotoxic effect of various patterns of circadian or continuous 5-FU delivery. The results provide a framework to account for experimental and clinical observations, and for helping us to predict optimal modes of drug delivery in cancer chronotherapy. By explaining the differential cytotoxicity of various circadian schedules of 5-FU delivery, the model clarifies the foundations of cancer chronotherapeutics. In view of its versatility and reduced number of parameters, the automaton model could readily be applied, *mutatis mutandis*, to probe the administration schedules of other types of anticancer medications active on other phases of the cell cycle, which could serve as the basis for the development of new cancer chronotherapies using advanced drug-delivery concepts and technologies.

Acknowledgments

We acknowledge support from the *Fonds de la Recherche Scientifique Médicale* (F.R.S.M., Belgium) through grant #3.4636.04, and from the European Union through the Network of Excellence BioSim, contract no. LSHB-CT-2004-005137. This study was performed while one of the authors (AG) held a *Chaire Internationale de Recherche Blaise Pascal de l'Etat et de la Région Ile-de-France, gérée par la Fondation de l'Ecole Normale Supérieure* in the Institute of Genetics and Microbiology at the University of Paris-Sud 11, Orsay, France.

Appendix A. Parameter values and initial conditions for simulations of the cell cycle model

Table 1
Parameter values and initial conditions considered in the various figures based on numerical simulations of the cell cycle automaton model. Except for Fig. 9(F), all figures were established for a uniform distribution of durations of cell cycle phases around a mean value, with variability *V*. « Entrained » means that the cell cycle is driven by the circadian clock through the circadian variation of Wee1 and Cdk1 (see text for further details). The cell cycle of 22 h duration consists of the following mean durations for the successive phases: G1 (9 h), S (11 h), G2 (1 h), and M (1 h). For the cell cycle of 26 h, the mean phase durations are: G1 (11 h), S (11 h), G2 (3 h), and M (1 h)

Cycle length	22 h		22 h		22 h (lognormal distribution)		26 h		26 h	
Entrained	−		+		+		−		+	
Initial conditions	15,000 cells in G1		10,000 cells at steady state*		10,000 cells at steady state*		15,000 cells in G1		10,000 cells at steady state**	
Variability (*V*)	Probability of quitting the cycle (min^{-1})	Figures	Probability of quitting the cycle (min^{-1})	Figures	Probability of quitting the cycle (min^{-1})	Figure	Probability of quitting the cycle (min^{-1})	Figure	Probability of quitting the cycle (min^{-1})	Figure
0%	0.0005380	*6A, 6C, 6E*	0. 0004925	*6B, 6D, 6F, 9E*	0. 0004930	*9F*	0. 0004550		0. 0004905	
5%	0. 0005380	*3A, 6A, 6C, 6E, 10A, 10C, 11A, 11C*	0. 0004925	*3B, 6B, 6D, 6F, 7A, 7C, 8A–D, 8I, 9E, 10B, 10D, 11B, 11D*	0. 0004930	*9F*	0. 0004550		0. 0004905	
10%	0. 0005380	*6A, 6C, 6E*	0. 0004925	*6B, 6D, 6F, 9E*	0. 0005180	*9F*	0. 0004550		0. 0004905	
15%	0. 0005380	*3C, 5A, 6A, 6C, 6E, 10A, 10B, 11A, 11B*	0. 0005150	*3D, 5C, 6B, 6D, 6F, 7B, 7D, 8E–H, 8J, 9E, 10C–D, 11C–D*	0. 0005280	*9F*	0. 0004550	*5B*	0. 0004830	*5D*
20%	0. 0005380	*6A, 6C, 6E*	0. 0005230	*6B, 6D, 6F, 9E*	0. 0005345	*9F*	0. 0004550		0. 0004730	

*Steady-state proportions of cells: 49.14% in G1, 44.22% in S, 3.90% in G2, 2.74% in M.

**Steady-state proportions of cells: 50.47% in G1, 37.20% in S, 9.84% in G2, 2.50% in M.

References

[1] L. Fu, H. Pelicano, J. Liu, P. Huang, C.C. Lee, The circadian gene Period2 plays an important role in tumor suppression and DNA damage response in vivo, Cell 111 (2002) 41–50.

[2] E. Filipski, V.M. King, X. Li, T.G. Granda, M.C. Mormont, X. Liu, B. Claustrat, M.H. Hastings, F. Levi, Host circadian clock as a control point in tumor progression, J. Natl. Cancer Inst. 94 (2002) 690–697.

[3] T. Matsuo, S. Yamaguchi, S. Mitsui, A. Emi, F. Shimoda, H. Okamura, Control mechanism of the circadian clock for timing of cell division in vivo, Science 302 (2003) 255–259.

[4] J. Hirayama, L. Cardone, M. Doi, P. Sassone-Corsi, Common pathways in circadian and cell cycle clocks: light-dependent activation of Fos/AP-1 in zebrafish controls CRY-1a and WEE-1, Proc. Natl. Acad. Sci. U. S. A. 102 (2005) 10194–10199.

[5] A.B. Reddy, G.K.Y. Wong, J. O'Neill, E.S. Maywood, M.H. Hastings, Circadian clocks: neural and peripheral pacemakers that impact upon the cell division cycle, Mutat. Res. 574 (2005) 76–91.

[6] R. Smaaland, Circadian rhythm of cell division, Prog. Cell Cycle Res. 2 (1996) 241–266.

[7] G.A. Bjarnason, R. Jordan, Circadian variation of cell proliferation and cell cycle protein expression in man: clinical implications, Prog. Cell Cycle Res. 4 (2000) 193–206.

[8] G.A. Bjarnason, R.C.K. Jordan, P.A. Wood, Q. Li, D.W. Lincoln, R.B. Sothern, W.J.M. Hrushesky, Y. Ben-David, Circadian expression of clock genes in human oral mucosa and skin, Am. J. Pathol. 158 (2001) 1793–1801.

[9] T.G. Granda, X.H. Liu, R. Smaaland, N. Cermakian, E. Filipski, P. Sassone-Corsi, F. Lévi, Circadian regulation of cell cycle and apoptosis proteins in mouse bone marrow and tumor, FASEB J. 19 (2005) 304–306.

[10] C. Focan, Circadian rhythms and cancer chemotherapy, Pharmacol. Ther. 67 (1995) 1–52.

[11] F. Lévi, Chronopharmacology of anticancer agents, in: P.H. Redfern, B. Lemmer (Eds.), Handbook of Experimental Pharmacology, Physiology and Pharmacology of Biological Rhythms, vol. 125, Springer-Verlag, Berlin, 1997, pp. 299–331.

[12] F. Lévi, Circadian chronotherapy for human cancers, Lancet Oncol. 2 (2001) 307–315.

[13] F. Lévi, From circadian rhythms to cancer chronotherapeutics, Chronobiol. Int. 19 (2002) 1–19.

[14] M.C. Mormont, F. Lévi, Cancer chronotherapy: principles, applications, and perspectives, Cancer 97 (2003) 155–169.

[15] A. Goldbeter, D. Claude, Time-patterned drug administration: Insights from a modeling approach, Chronobiol. Int. 19 (2002) 157–175.

[16] A. Goldbeter, Biochemical Oscillations and Cellular Rhythms, Cambridge Univ. Press, Cambridge, UK, 1996.

[17] J.J. Tyson, B. Novak, Regulation of the eukaryotic cell cycle: molecular antagonism, hysteresis, and irreversible transitions, J. Theor. Biol. 210 (2001) 249–263.

[18] B. Novak, J.J. Tyson, A model for restriction point control of the mammalian cell cycle, J. Theor. Biol. 230 (2004) 563–579.

[19] Z. Qu, W.R. MacLellan, J.N. Weiss, Dynamics of the cell cycle: checkpoints, sizers, and timers, Biophys. J. 88 (2003) 3600–3611.

[20] J.A. Smith, L. Martin, Do cells cycle? Proc. Natl. Acad. Sci. U. S. A. 70 (1973) 1263–1267.

[21] R.F. Brooks, D.C. Bennett, J.A. Smith, Mammalian cell cycles need two random transitions, Cell 19 (1980) 493–504.

[22] S.J. Cain, P.C. Chau, Transition probability cell cycle model. I. Balanced growth, J. Theor. Biol. 185 (1997) 55–67.

[23] J. Halloy, B.A. Bernard, G. Loussouarn, A. Goldbeter, Modeling the dynamics of human hair cycles by a follicular automaton, Proc. Natl. Acad. Sci. U. S. A. 97 (2000) 8328–8333.

[24] J. Halloy, B.A. Bernard, G. Loussouarn, A. Goldbeter, The follicular automaton model: effect of stochasticity and of synchronization of hair cycles, J. Theor. Biol. 214 (2002) 469–479.
[25] G. Metzger, C. Massari, M.C. Etienne, M. Comisso, S. Brienza, Y. Touitou, G. Milano, G. Bastian, J.L. Misset, F. Levi, Spontaneous or imposed circadian changes in plasma concentrations of 5-fluorouracil coadministered with folinic acid and oxaliplatin: relationship with mucosal toxicity in patients with cancer, Clin. Pharmacol. Ther. 56 (1994) 190–201.
[26] R. Zhang, Z. Lu, T. Liu, S.-J. Soong, R.B. Diasio, Relationship between circadian-dependent toxicity of 5-fluorodeoxyuridine and circadian rhythms of pyrimidine enzymes: possible relevance to fluoropyrimidine chemotherapy, Cancer Res. 53 (1993) 2816–2822.
[27] F. Lévi, R. Zidani, J.M. Vannetzel, B. Perpoint, C. Focan, R. Faggiuolo, P. Chollet, C. Garufi, M. Itzhaki, L. Dogliotti, et al., Chronomodulated versus fixed-infusion-rate delivery of ambulatory chemotherapy with oxaliplatin, fluorouracil, and folinic acid (leucovorin) in patients with colorectal cancer metastases: a randomized multi-institutional trial, J. Natl. Cancer Inst. 86 (1994) 1608–1617.
[28] F. Lévi, R. Zidani, J.L. Misset, Randomised multicentre trial of chronotherapy with oxaliplatin, fluorouracil, and folinic acid in metastatic colorectal cancer. International Organization for Cancer Chronotherapy, Lancet 350 (1997) 681–686.
[29] M.V. Blagosklonny, A.B. Pardee, Review. Exploiting cancer cell cycling for selective protection of normal cells, Cancer Res. 61 (2001) 4301–4305.
[30] J. Clairambault, P. Michel, B. Perthame, Circadian rhythm and tumour growth, C. R. Acad. Sci. (Paris) Ser. 1 342 (2006) 17–22.
[31] C. Basdevant, J. Clairambault, F. Lévi, Optimisation of time-scheduled regimen for anti-cancer drug infusion, Math. Model. Numer. Anal. 39 (2005) 1069–1086.
[32] B.F. Dibrov, A.M. Zhabotinsky, Y.A. Neyfakh, M.P. Orlova, L.I. Churikova, Mathematical model of cancer chemotherapy. Periodic schedules of phase-specific cytotoxic agent administration increasing the selectivity of therapy, Math. Biosci. 73 (1985) 1–31.
[33] B.F. Dibrov, Resonance effect in self-renewing tissues, J. Theor. Biol. 192 (1998) 15–33.
[34] Z. Agur, The effect of drug schedule on responsiveness to chemotherapy, Ann. N.Y. Acad. Sci. 504 (1986) 274–277.
[35] Z. Agur, R. Arnon, B. Schechter, Reduction of cytotoxicity to normal tissue by new regimens of cell-cycle phase-specific drugs, Math. Biosci. 92 (1988) 1–15.
[36] Z. Agur, R. Arnon, B. Sandak, B. Schechter, Zidovudine toxicity to murine bone marrow may be affected by the exact frequency of drug administration, Exp. Hematol. 19 (1991) 364–368.
[37] P. Ubezio, G. Tagliabue, B. Schechter, Z. Agur, Increasing 1-β-D-arabinofuranosylcytosine efficacy by scheduled dosing intervals based on direct measurements of bone marrow cell kinetics, Cancer Res. 54 (1994) 6446–6451.
[38] G.F. Webb, Resonance phenomena in cell population chemotherapy models, Rocky Mt. J. Math. 20 (1990) 1195–1216.
[39] L.K. Andersen, M.C. Mackey, Resonance in periodic chemotherapy: a case study of acute myelogenous leukemia, J. Theor. Biol. 209 (2001) 113–130.